

ARTICLE

Optimization of the thermal mending process in epoxy/cyclic olefin copolymer blends

Andrea Dorigato^{1,2}  | Haroon Mahmood^{1,2}  | Alessandro Pegoretti^{1,2} 

¹Department of Industrial Engineering,
University of Trento, Trento, Italy

²National Interuniversity Consortium of
Materials Science and Technology
(INSTM), Florence, Italy

Correspondence

Haroon Mahmood and Alessandro
Pegoretti, Department of Industrial
Engineering, University of Trento, Via
Sommarive 9 38123 Trento (Italy).
Email: haroon.mahmood@unitn.it
(H. M.) and alessandro.pegoretti@unitn.
it (A. P.)

Funding information

Fondazione Cassa di Risparmio di Trento
e Rovereto (IT), Grant/Award Number:
2017.0389

Abstract

Cyclic olefin copolymer (COC) is utilized as thermoplastic healing agent in an epoxy resin and the effect of mending temperature on the healing of resulting materials is investigated. Blends are prepared by adding 20 and 30 wt% COC powder in the epoxy resin. They are thermo-mechanically characterized and fractured samples are thermally mended at various temperatures to evaluate the healing efficiency of the repaired samples. Optical microscopy reveals a homogenous dispersion of COC domains within epoxy matrix, while thermogravimetric analysis shows improved thermal stability of the samples. The immiscibility of the two phases in the blends lead to a decrease of the mechanical properties under flexural and tensile loading modes with respect to neat epoxy. The fracture toughness increases upon COC addition at elevated amounts. Healing efficiency values up to more than 80% are obtained at the lowest investigated temperature of 145°C for samples with 30 wt% of COC.

KEYWORDS

blends, mechanical properties, structure-property relationships, thermal properties, thermosets

1 | INTRODUCTION

Among the polymeric materials, epoxy resins are mostly used in many engineering applications like composites, printed circuit boards, coatings, or adhesives. Its importance stems from the fact that it possesses higher chemical resistance, good electrical properties, increased mechanical, and fatigue resistance. However, the brittle nature of epoxy resins makes them vulnerable to microcracks formed during the service. These cracks might gradually lead to a catastrophic failure of the structure. Hence the importance of such issue has led to the development of epoxy-based systems that could lead to spontaneous healing of epoxy resin to “restore” some mechanical properties of the structure.

Epoxy based blends and composites have been actively researched in the past century not only for structural applications, but also for smart multifunctional materials.^{1–5} For almost a couple of decades, scientists and researchers around the world have been pursuing

with great interest the development of self-healable polymer and composites.^{6–11} The first work reported by White et al.¹² in this field involved the use of extrinsic elements in the bulk polymer, that is, capsules and a catalyst for the self-healing of cracks. Up to now, different approaches have been considered for the healing of bulk polymers and/or composites, and the repairing potential was evaluated by investigating the crack propagation resistance before and after the mending process.¹³ Systems having the ability to heal themselves are classified as extrinsic self-healing systems, that is, no external stimulus is required to perform the mending process.¹⁴ Healing agents added in such systems may be contained in capsules or capillaries which upon breaking (mechanical damage) release the healing agent to perform the mending. In order to perform this operation, a catalyst contained within capsules or capillaries can be added to polymer matrices. Although these systems could provide autonomous damage repair, the main limitation is

represented by the fact that such reparability is possible only one time, that is, they do not allow multiple healing events, because of the thermosetting nature of the healing agents. Moreover, the complications involved in the creation of microspheres or vascular networks render the fabrication of such systems quite complicated. In addition, the limited thermal and environmental stability of microcapsules could represent another strong limitation.¹⁵ On the other hand, intrinsic systems provide the opportunity to heal themselves several times, due to the presence of constituents which could undergo a molecular reentanglement process.¹³ The reentanglement across the crack front of the broken surfaces usually occurs by the application of external energy, like heat and pressure. The applied temperature must be above the glass transition temperature (T_g) or the melting temperature (T_m) of the healing agent, depending if it is amorphous or semicrystalline, respectively. For instance, intrinsic systems based on Diels-Alder (DA) and retro-DA (rDA) reversible reactions allowed the thermal activation at elevated temperatures (from 100 to 150°C) of healing agents,¹⁶ applied for multiple self-healing in epoxy (EP) or polyamide (PA) systems.

The investigation of solid-state healing agents for mending thermosetting matrices has become a hot topic in recent years. Thermoplastic materials that could soften/melt upon heating have recently gained particular interest in this field. In this case, the mending mechanism involves the interdiffusion of polymeric molecules due to the application of heat and pressure on the cracked zones.¹⁷ If the crack is completely filled by the softened thermoplastic and the chemical compatibility between the two polymers is good, an effective healing can be achieved. Ideally, a thermoplastic polymeric healing agent should satisfy the following three requirements: (i) low softening/melting point, with a viscosity low enough to be able to flow in the crack, (ii) chemical functional groups reactive in nature with the host matrix, and (iii) appropriate adhesive properties with the host matrix for an effective crack mending process.¹⁸

The effectiveness of various polymers as possible effective healing agents has been recently investigated.^{19–25} A pioneering work in this field was presented by Hayes et al.,¹⁹ in which the use of a polybisphenol-A-co-epichlorohydrin based thermoplastic as a healing agent in an epoxy resin was presented. Such system showed a healing efficiency under impact conditions of 65%, if the healing agent was added at a concentration of 7.5 wt%. Meure et al.²⁶ proved that a dispersion of particles polyethylene-co-methacrylic acid (EMAA) in an epoxy resin promoted about 85% of recovery of the critical stress intensity factor. Pingkarawat et al.²⁷ used mode I fracture toughness test to evaluate the healing efficiency of different thermoplastic polymers in epoxy-carbon fiber

composites. In particular, EMAA dispersed in the form of particles in the composites showed a healing efficiency of about 150%, due to the reactive nature of EMAA particles. In another work of Wang et al.,²¹ EMAA was used in the form of rectangular sheets between the epoxy-carbon fiber prepreg plies, and the healing was performed at 150°C for 30 min. Mode I fracture toughness tests on double cantilever beam (DCB) specimens showed that a healing efficiency of 88% could be achieved in epoxy-carbon fiber composites. Luo et al.²³ demonstrated for the first time the use of poly(ϵ -caprolactone) (PCL) as a healing agent in an epoxy matrix. The formation of a miscible blend composed of 15.5 wt% PCL allowed the achievement of healing efficiencies of more than 100% on single edge notched beam (SENB) specimens healed at 190°C for 8 min. Rodriguez et al.²⁴ utilized a thermoplastic PCL as healing agent in a cross-linked matrix, obtaining a healing efficiency of at least 95% with a PCL concentration of 25 wt%. By using a similar approach, Wei et al. used PCL as healing agent for an epoxy based shape memory polymer,²⁸ demonstrating that the healing temperature could play a key role in the mending process. At around 144°C (i.e. 80°C above the melting point of PCL), the reported healing efficiency was about 78%.

In the major part of the papers available in the literature, semi-crystalline thermoplastic polymers, having a melting point lower than the T_g of host matrix, have been considered as healing agents. Very recently, Mahmood et al.²⁹ revealed the possibility of using an amorphous thermoplastic as a healing agent for thermosetting matrices. In that work, an amorphous cyclic olefin copolymer (COC) having a T_g of 79°C was dispersed in the form of particles in an epoxy matrix for structural applications ($T_g = 84^\circ\text{C}$), and healing efficiency levels of around 100% were obtained with a COC concentration of about 30–40 wt%. In this work, thermal mending on SENB specimens was performed at 190°C for 1 h, applying a pressure of 15 MPa. This amorphous matrix was selected on the basis of the previous works of our group on COC based nanocomposites³⁰ and foams.^{31–33} Compared to similar works in which semi-crystalline thermoplastic polymer were utilized as healing agent,^{19,26,34–36} the applied mending parameters in that paper were rather heavy. Considering the economical applicability of this process, elevated temperature and pressure levels in the thermal mending could strongly limit its applicability. Moreover, in these conditions a partial thermal degradation of the polymer matrix can occur, with a deterioration of its mechanical performances. If applied to fiber reinforced laminates, these mending parameters could also promote the distortion of the fabrics in the composites. In another work of Mahmood et al.,³⁷ COC/epoxy matrices were also

utilized to prepare thermally mendable unidirectional carbon fibers (CF) reinforced laminates. Laminated samples, having a COC content of 30 wt% within the matrix, were healed at 190°C applying a considerably lower pressure level (i.e. 0.5 MPa). Mode I fracture toughness tests on DCB specimens showed a healing efficiency of ~270% in the first healing cycle, which decreased to 100% in the second healing cycle.

In the last decades, polymer blends (including epoxy resin) have been investigated by many researchers, with the aim to improve the thermo-mechanical properties of the neat matrices and induce functional properties.^{6,38–41} Examples of such blends are represented by toughened elastomers, impact-resistant plastics and polymer-impregnated concrete etc.^{42–45} However, polymer blending requires not only the know-how of the chemical and physical properties of polymers, but also of other key aspects like processing, miscibility, compatibilization, rheology, morphology and performance during the service life of these materials.^{46,47}

On the basis of the above considerations, in the present work, an optimization of the thermal mending process in epoxy/COC polymer blends has been investigated. Thermo-mechanical characterization of the prepared materials was performed to compare the prepared blends. In particular, four thermal mending temperatures (i.e. 145, 160, 175, 190°C) along with an applied compressive pressure of 0.5 MPa have been selected in this work. This was done in order to compare the healing efficiencies obtained by different mending parameters.

2 | EXPERIMENTAL

2.1 | Materials

A bicomponent epoxy system consisting of an epoxy base and aminic hardener, EC157 and W342, respectively (initial viscosity at 25°C: 300–700 mPas), provided by Elantas Europe Srl (Collecchio, Italy), was used as a thermosetting matrix. TOPAS® 8007 COC granules, supplied by Ticona (Kelsterbach, Germany), were used as a healing agent in the epoxy matrix. It is a thermoplastic polymer constituted by 65 wt% ethylene and 35 wt% norbornene (melt flow index at 190°C and 2.16 kg = 1.7 g/10 min, density = 1.02 g/cm³, T_g = 78°C). All materials were used as received without any further treatment.

2.2 | Preparation of the samples

COC was added in the form of grinded particles in epoxy matrix. Cryogenic milling of COC granules was

performed by using a IKA Labortechnik M20 (IKA Werke GmbH, Germany) grinding machine. Sieving of the grinded particles was carried to obtain a final granulometry below 300 μm. Mixtures of epoxy base and COC particles were prepared by shear mixing at 3000 rpm for 1 h at 50°C. Degassing of the epoxy/COC mixture was performed through a desiccator connected to a vacuum pump for 1 h. After the degassing, the hardener was introduced in the mixture at a base to hardener ratio of 100:30. The resulting blend was mixed for 5 min at 1000 rpm, and another degassing process with a total duration of 20 minutes was then carried out. The mixture was then poured in respective silicon molds with specific specimen size and shape for mechanical testing (according to testing requirements as discussed later) and cured for 24 h at 23°C + 15 h at 60°C, as suggested by the producer of the epoxy system. In this way, neat epoxy samples and epoxy/COC blends with a COC content of 20 and 30 wt% were prepared. These COC concentrations were selected on the basis of the results of a previous paper of our group on these systems.²⁹ The list of the prepared matrices with the relative concentration of the constituents is reported in Table 1.

Only EP/COC blends were thermally treated at different temperatures, that is, 145, 160, 175, and 190°C for 1 h in order to investigate the changes in physical, thermal and mechanical properties of the blends. Selection of these temperatures was based on the aim of optimizing the thermal mending properties which will be discussed later. Hence, in this work, untreated samples were designated with the letter u (untreated) whereas the thermally treated samples were denoted by the notation t followed by the temperature of thermal treatment, for example, t¹⁴⁵-EP/COC20, and so forth. Table 2 summarizes the list of samples with the relative notation.

Moreover, two healing cycles were performed on the untreated samples at the above-mentioned temperatures. A screw driven mold was used to put in contact the broken parts, applying a compressive stress of 500 kPa. The pressure level was selected according to the indications reported in our previous work on composites laminates with self-healing capability.³⁷ During the thermal mending process, a piece of the original blade used to create the notch in the specimens was placed exactly in the notch area, in order to maintain a starting crack. The healed samples were denoted as Ix or IIx, where I or II refers to the number of healing events performed, while “x” refers to the temperature at which healing was performed. In Table 3, the list of the repaired samples with the relative notation is summarized.

Representative pictures of the prepared epoxy/COC blends (both untreated and treated) at different COC concentrations is shown in Figure 1. Even if the both epoxy and COC are optically transparent polymers, the blend

Materials	Epoxy base (wt%)	Hardener (wt%)	COC (wt%)
EP	76.9	23.1	—
EP/COC20	61.5	18.5	20
EP/COC30	53.8	16.2	30

TABLE 1 Composition of the prepared epoxy/COC blends**TABLE 2** List of the prepared samples with the relative notation

	Treatment temperature (°C)	EP	EP/COC20	EP/COC30	COC
Untreated	—	u-EP	u-EP/COC20	u-EP/COC30	u-COC
Treated	145	—	t ¹⁴⁵ -EP/COC20	t ¹⁴⁵ -EP/COC30	—
Treated	160	—	t ¹⁶⁰ -EP/COC20	t ¹⁶⁰ -EP/COC30	—
Treated	175	—	t ¹⁷⁵ -EP/COC20	t ¹⁷⁵ -EP/COC30	—
Treated	190	—	t ¹⁹⁰ -EP/COC20	t ¹⁹⁰ -EP/COC30	—

with a content of 20 or 30 wt% are opaque. This is an indication of the relative immiscibility between the two polymeric phases and the consequent presence of interfaces that can scatter the light. Moreover, when the treatment temperature is increased, the color of the specimens gradually turns into an orange tint. As already seen in our previous work on these systems,²⁹ this effect is associated to the thermal oxidation of the epoxy resin.⁴⁸ Therefore, a decrease of the mending temperature could be important to retain the pristine properties of the epoxy matrix even after prolonged thermal exposure.

3 | EXPERIMENTAL TECHNIQUES

3.1 | Microstructural and chemical properties

The microstructure of u-EP/COC samples was analyzed by using a Zeiss Axiophot optical microscope (Carl Zeiss AG, Germany) equipped with a Leica DC300 digital camera (Leica Microsystems Ltd., Switzerland). Before to be

observed, the specimens were polished by using abrasive grinding paper with grit size P240, P500, P800, P1200, and P4000, sequentially. Specimens were then polished by using an aqueous suspension of diamond particles with a granulometry of 3 and 1 μm , progressively.

ATR-FTIR spectroscopy was performed through a Perkin Elmer Spectrum One machine both on untreated and treated EP/COC blends, in order to analyze the effect of thermal treatment on the functional groups. The analyses were performed in a wavenumber range from 650 to 4000 cm^{-1} . The specimens were placed on the top of the ATR crystal and a specific force was applied on the specimen. The obtained spectra contained peaks having varying percent transmission as a function of applied infrared wavenumber (cm^{-1}).

3.2 | Thermal properties

Differential scanning calorimetry (DSC) was performed by a Mettler DSC30 calorimeter (Mettler-Toledo GmbH, USA). For every specimen, a first heating stage

TABLE 3 List of the repaired samples with the relative notation

Healing cycle	Thermal mending temperature (°C)	EP/COC20	EP/COC30
1	145	I ¹⁴⁵ _u -EP/COC20	I ¹⁴⁵ _u -EP/COC30
1	160	I ¹⁶⁰ _u -EP/COC20	I ¹⁶⁰ _u -EP/COC30
1	175	I ¹⁷⁵ _u -EP/COC20	I ¹⁷⁵ _u -EP/COC30
1	190	I ¹⁹⁰ _u -EP/COC20	I ¹⁹⁰ _u -EP/COC30
2	145	II ¹⁴⁵ _u -EP/COC20	II ¹⁴⁵ _u -EP/COC30
2	160	II ¹⁶⁰ _u -EP/COC20	II ¹⁶⁰ _u -EP/COC30
2	175	II ¹⁷⁵ _u -EP/COC20	II ¹⁷⁵ _u -EP/COC30
2	190	II ¹⁹⁰ _u -EP/COC20	II ¹⁹⁰ _u -EP/COC30

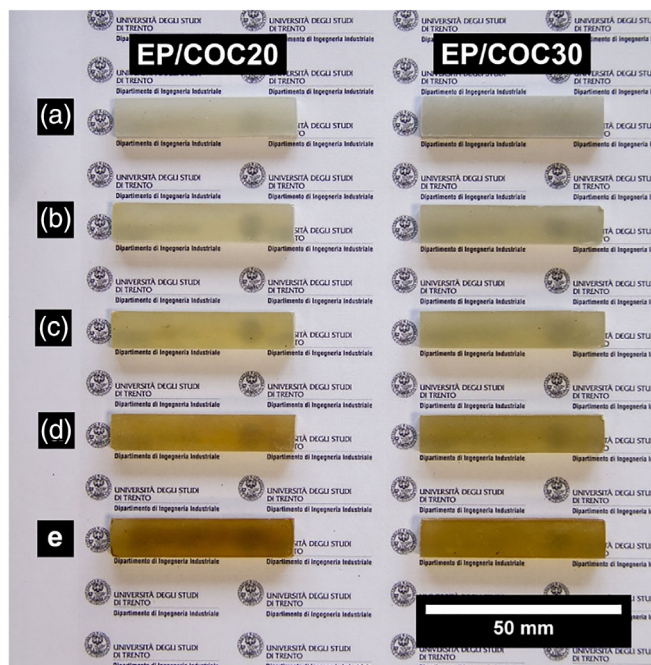


FIGURE 1 Representative images of the prepared EP/COC blends. Untreated samples (a), samples treated at 145°C (b), 160°C (c), 175°C (d) and 190°C (e). COC, cyclic olefin copolymer; EP, epoxy [Color figure can be viewed at [wileyonlinelibrary.com](#)]

from 0 to 150°C was followed by a cooling stage from 150 to 0°C and by a second heating stage from 0 to 150°C. The tests were performed at a heating rate of 10°C·min⁻¹, under a nitrogen flow of 100 ml·min⁻¹. In this way, the glass transition temperature (T_g) of both COC and the epoxy phases were determined. The thermal stability of the blends was evaluated by thermogravimetric analysis (TGA). Tests were performed through a Mettler TG50 machine (Mettler-Toledo GmbH, USA), applying a temperature ramp from 35 to 700°C at a heating rate of 10°C·min⁻¹, under a constant nitrogen flow of 100 ml·min⁻¹. In this way, the onset degradation temperature (T_{onset}), the temperature associated to a mass loss of 50% ($T_{50\%}$), the decomposition temperatures of epoxy matrix (T_{dEP}) and COC (T_{dCOC}), considered as the temperatures of the maximum mass loss rate, and the residual mass at 700°C (m_{700}), were determined.

3.3 | Mechanical properties

The mechanical properties of the samples were evaluated under quasi-static tensile mode on ISO 527 1BA dogbone specimens by an Instron® 5969 tensile testing machine (ITW Test & Measurement and Equipment, USA) equipped with a 50 kN load cell. At least five specimens

were tested for each sample. Elastic modulus was determined through tests at a crosshead speed of 0.25 mm·min⁻¹, performed up to a strain level of 1%. An Instron 2620–601 extensometer with a gage length of 12.5 mm was used to measure the strain. The elastic modulus was determined as a secant value between strain levels of 0.05% and 0.25%. For the determination of the ultimate properties (stress and strain at break), the tests were performed at a constant crosshead speed of 1 mm·min⁻¹, without using the extensometer.

Samples were also tested under flexure (three-point bending) according to ASTM D790 standard. Rectangular specimens with dimension of 65 × 12.5 × 3 mm³ were tested at a crosshead speed of 1.3 mm·min⁻¹, setting a span length of 48 mm. At least five specimens for each composition were tested.

3.4 | Fracture toughness and healing efficiency

The fracture toughness was evaluated according to the procedure described in the ASTM D5045 standard. The tests were carried out on SENB specimens, having dimensions of 44 × 10 × 5 mm³ and an initial notch length of 5 mm. At least five specimens were tested for each composition. Tests were performed by using an Instron® 5969 electromechanical testing machine (ITW Test & Measurement and Equipment, USA) at a crosshead speed of 10 mm·min⁻¹. From the maximum load sustained by the samples (P), it was possible to determine the critical stress intensity factor (K_{IC}), according to the expressions reported in Equations (1) and (2)⁴⁹:

$$K_Q = \frac{P}{BW^{3/2}} f(x) \quad (1)$$

$$f(x) = 6x^{1/2} \frac{1.99 - x(1-x)(2.15 - 3.93x + 2.7x^2)}{(1+2x)(1-x)^{3/2}} \quad (2)$$

where P is the maximum load sustained by the samples, B and W are, respectively, the thickness and the width of the samples, and $f(x)$ is a calibration factor, with $x = a/W$. Moreover, from the integration of the load-displacement curves and evaluation of system compliance (see ASTM standard D5045), also the critical strain energy release rate (G_{IC}) values were obtained, according to the expression reported in Equation (3)⁴⁹:

$$G_{IC} = \frac{\Delta U}{WB\phi} \quad (3)$$

where ΔU is the difference of the total energy absorbed by the sample and the energy absorbed in the indentation tests, and Φ is an energy calibration factor, whose expression is reported in ASTM D5045 standard.

The healing efficiency of the prepared samples was determined by performing a thermal mending of the broken SENB specimens. As discussed before, four different temperatures (from 145 to 190°C) were considered in this work to evaluate the minimum temperature required for thermal mending of EP/COC systems.

K_{IC} and G_{IC} were calculated also for the repaired specimens, tested under the same conditions. By the ratio of K_{IC} value of the healed samples ($K_{IC,H}$) and of the virgin ones ($K_{IC,UV}$), the apparent healing efficiency (η) values were determined, as reported in Equation (4)²⁹:

$$\eta = \frac{K_{IC,H}}{K_{IC,UV}} \quad (4)$$

Considering the elevated temperatures (at least 65°C above T_g of epoxy) applied for the thermal mending of the specimens, it was necessary to determine the fracture behavior of the thermally treated virgin samples, as reported in previous work on similar systems.²⁹ A real healing efficiency value (η') was then calculated as the ratio between the K_{IC} value of the healed samples ($K_{IC,H}$) and that of the virgin thermally treated ones ($K_{IC,TV}$), as reported in Equation (5)²⁹:

$$\eta' = \frac{K_{IC,H}}{K_{IC,TV}} \quad (5)$$

In this way, it was possible to separate the effect induced by the thermal mending process to that provided by the thermal treatment on the polymer matrix.

In order to better understand the morphological aspects related to the mending process, a Zeiss Axiophot microscope, equipped with a Leica DDC295 digital camera, was utilized to observe the polished surface of the thermally mended samples at different magnification levels. The same equipment was also utilized to observe the fracture front of the samples healed at different temperatures, that were broken in fracture tests performed under three-point bending configuration. In this way, it was possible to have detailed information on the crack propagation mode and on the subsequent healing mechanism.

4 | RESULTS AND DISCUSSION

4.1 | Microstructural and chemical properties

The dispersion of COC particles in the u-EP/COC20 sample can be evaluated in the optical microscope pictures

reported in Figure 2. The optical micrographs show a rather homogenous dispersion of COC particles having irregular shape within the epoxy matrix. The mean size of COC domains is around 180 μm . Considering that solid COC powder was dispersed in the liquid epoxy precursors, it is clear that a completely phase-separated microstructure is formed. Apparently, no interfacial debonding can be found at all the magnification levels, which hints a good adhesion between epoxy and COC (as pointed by the arrows in the figure). A similar microstructure was also detected for the EP/COC30 blend (not reported here for the sake of brevity).

In Figure 3(a) the FTIR spectra of neat epoxy and COC samples with the prepared blends repaired at 190°C are compared. Neat COC shows two double peaks: the first at 2944 and 2922 cm^{-1} , the second at 2867 and 2853 cm^{-1} . These peaks are related to the stretching of the CH_2 and CH_3 groups, respectively. These same reflections are present as single peaks also in the spectrum of epoxy resin. In this figure it can be clearly seen a broad peak related to $-\text{OH}$ stretching in epoxy resin at 3330 cm^{-1} , with no counterparts in the COC spectrum. The comparison between the spectra of neat EP and COC samples and those of the blends healed at 190 °C shows a decrease in transmittance in correspondence of the peaks at 2930 and 2850 cm^{-1} . The slightly higher peak intensity for the EP/COC30 blend is due to the higher fraction of healing agent. Peaks at wavenumber of 1716 and 1652 cm^{-1} , associated to $\text{C}=\text{O}$ stretching, appear only in the spectra of repaired blends. This is probably due to the partial oxidation of these samples during the thermal treatment at 190°C for 1 h. This evidence could justify the change in the color of the thermally treated blends evidenced in Figure 1. Through FTIR spectroscopy, the effect of thermal treatment on the blends was also investigated. The spectra associated to EP/COC20 samples treated at various temperatures are compared with that of the untreated one in Figure 3(b). From these spectra it can be noted that the peaks associated to the epoxide reactive groups at about 3300 and 932 cm^{-1} exhibit a higher transmittance in the case of samples treated at higher temperatures. This implies that the curing process is more effective at elevated treatment temperatures. The increase of the crosslinking degree detected with FT-IR analysis could also affect the mechanical properties of the thermally treated blends.

4.2 | Thermal properties

The thermal behavior of the investigated blends was analyzed through DSC analysis. The obtained thermograms during the first and second heating stage of untreated

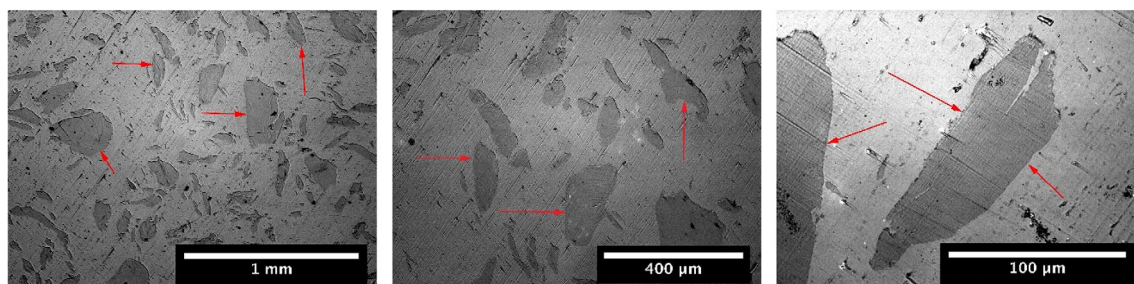


FIGURE 2 Optical microscope images of the polished surfaces of epoxy/COC20 at different magnification levels. COC, cyclic olefin copolymer [Color figure can be viewed at wileyonlinelibrary.com]

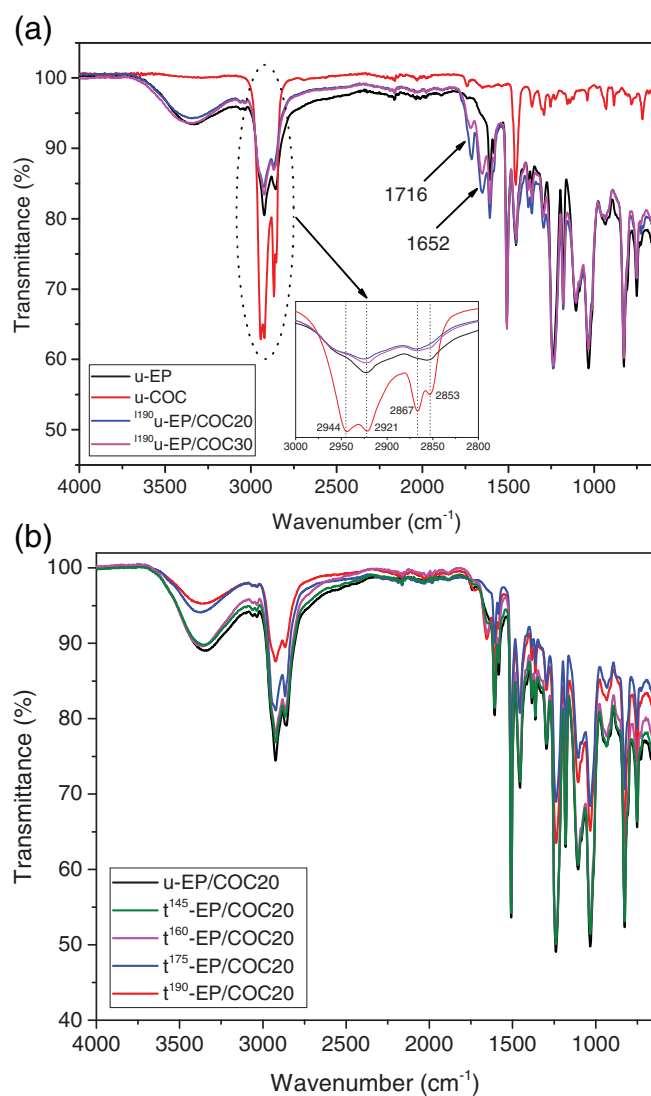


FIGURE 3 (a) FTIR spectra of u-EP, u-COC, 1190 u-EP/COC20 and 1190 u-EP/COC30 samples. (b) FTIR spectra of EP/COC20 samples (untreated and thermally treated at different temperatures). COC, cyclic olefin copolymer; EP, epoxy [Color figure can be viewed at wileyonlinelibrary.com]

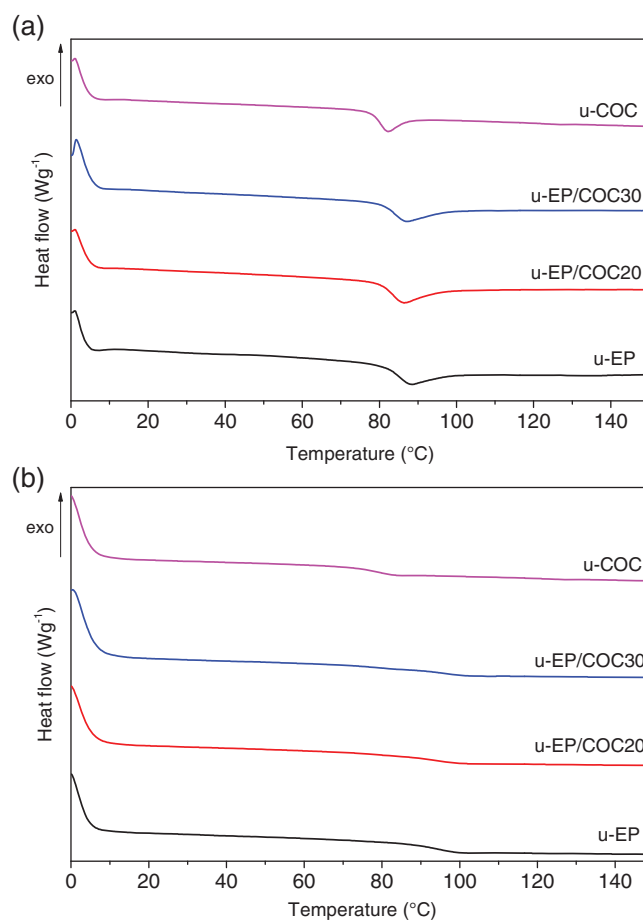


FIGURE 4 DSC thermograms of neat epoxy, neat COC, and epoxy/COC blends. (a) First heating stage and (b) second heating stage. COC, cyclic olefin copolymer; DSC, differential scanning calorimetry; EP, epoxy [Color figure can be viewed at wileyonlinelibrary.com]

epoxy, COC, EP/COC20 and EP/COC30 are compared in Figure 4 (a-b), while the glass transition temperatures (T_g) of the epoxy and COC phases are summarized in Table 4. In the first heating cycle, the epoxy resin shows

Samples	T_g^1 EP (°C)	T_g^1 COC (°C)	T_g^2 EP (°C)	T_g^2 COC (°C)
u-EP	84.5	—	93.6	—
u-EP/COC-20	83.1	—	93.3	—
u-EP/COC-30	84.0	—	94.8	—
u-COC	—	79.8	—	78.7
t ¹⁴⁵ -EP/COC20	96.4	77.0	100.8	77.5
t ¹⁶⁰ -EP/COC20	84.3	—	89.9	—
t ¹⁷⁵ -EP/COC20	91.9	—	94.8	78.3
t ¹⁹⁰ -EP/COC20	98.1	76.2	98.1	77.5
t ¹⁴⁵ -EP/COC30	96.5	76.9	99.9	76.4
t ¹⁶⁰ -EP/COC30	96.3	76.8	100.5	75.5
t ¹⁷⁵ -EP/COC30	93.7	—	95.2	76.6
t ¹⁹⁰ -EP/COC30	95.3	77.3	100.1	78.0

TABLE 4 Results of DSC tests on neat epoxy, neat COC and the prepared epoxy/COC blends

Note: T_g^1 EP is the glass transition temperature of epoxy (first heating stage). T_g^1 COC is the glass transition temperature of COC (first heating stage). T_g^2 EP is the glass transition temperature of epoxy (second heating stage). T_g^2 COC is the glass transition temperature of COC (second heating stage).

a T_g of 84.5°C, while the glass-transition temperature in the second heating stage is higher than that evaluated in the first cycle (i.e., 93.6°C). This is associated to a higher cross-linking degree developed in the epoxy due to the thermal treatment during the first heating cycle. On the other hand, neat COC shows a slightly decreased glass transition temperature between first and second cycle. This effect, even if very limited, could be related to a slight degradation of COC during the first heating cycle. Being COC an amorphous material, it does not show crystallization peaks during cooling (not reported for the sake of brevity). Both in the first and in the second heating cycle, EP/COC20 and EP/COC30 blends show T_g values very close to those of epoxy, without any correlation with the COC concentration. The results of DSC tests on thermally treated samples are summarized in Table 4 (the thermograms of which are compared in supporting information Appendix S1). Also thermally treated samples show two distinct glass-transition temperatures in both first and second heating cycle, related to COC and epoxy resin. The glass-transition temperature of treated epoxy resin is systematically higher than that of untreated one, regardless to the treatment temperature. This occurs because of the increase of the crosslinking degree promoted by the thermal treatment. The T_g values for epoxy/COC blends are only slightly higher in the second cycle, thus suggesting that the curing process is almost complete upon the thermal treatment, even at low temperature (145 °C). On the other hand, the T_g values of COC remains almost constants between first and second heating cycle, and they are very similar to the T_g values reported for the u-COC sample.

Even in this case, there is no correlation between the COC content or the thermal treatment temperature and the T_g value of epoxy phase in the blends. It is therefore confirmed that the COC phase does not play any influence on the glass transition of the epoxy, suggesting that the interactions between the two phases are rather limited.

The thermograms of the residual mass and of the derivative of the mass loss as a function of the testing temperature for the untreated samples as measured from TGA tests are reported in Figure 5(a-b). The most important results are collected in Table 5. The first derivative of the residual mass shows two distinct peaks in the curves related to the blends: the first peak is due to the decomposition of epoxy resin, whereas the second one is due to the decomposition of COC. It can be clearly noticed that the values of T_{onset} , $T_{50\%}$ and T_{offset} increase with the COC concentration. Therefore, the introduction of the healing agent also increases the thermal stability of the blends. This is due to the fact that u-COC shows higher values of T_{onset} , $T_{50\%}$ and T_{offset} with respect to the neat epoxy sample. Even T_{dCOC} is about 100 °C higher than T_{dEP} . Moreover, the residue at 700 °C (m_{700}) of EP is 8.0%, and the addition of COC yields a m_{700} decrease down to 5.2% (EP/COC20) and to 5.5% (EP/COC30). This is because COC does not leave any residue upon thermal decomposition, as it completely evolves into volatile species. These results confirm the conclusion reported in our previous work on epoxy/COC blends.²⁹ The results of TGA tests on thermally treated EP/COC blends are reported in Table 5 (the thermograms of which are compared in supporting information). It can be immediately seen that the thermal treatment does not change significantly the

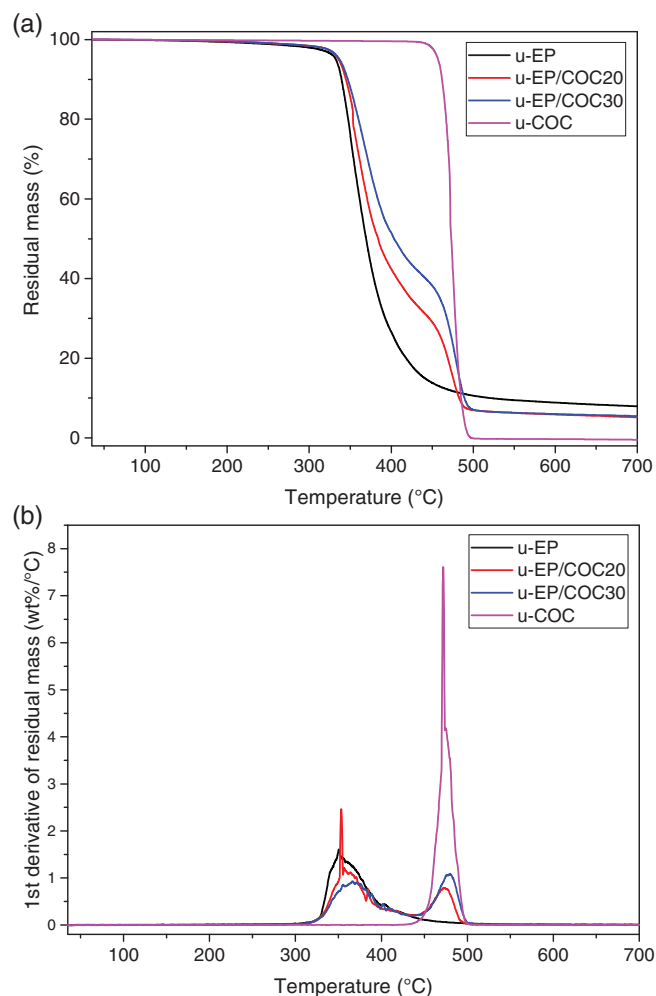


FIGURE 5 TGA tests on untreated epoxy, EP/COC blends, and COC samples. (a) Residual mass and (b) derivative of the mass loss as a function of the testing temperature. COC, cyclic olefin copolymer; EP, epoxy [Color figure can be viewed at wileyonlinelibrary.com]

degradation behavior of the blends, regardless to the temperature at which it is performed. T_{onset} and $T_{50\%}$ slightly increase in thermally treated samples, due to the further curing of epoxy resin, but all the tested samples show characteristic temperature variations in the range of 10 °C, and also the m_{700} values are very similar.

4.3 | Mechanical properties

The results of quasi-static and flexural tests on untreated samples are summarized in Table 6. It can be clearly seen that all mechanical properties (elastic modulus, stress and elongation at break) decrease with the COC introduction, especially at a concentration of 30 wt%. Even if the reduction of elastic modulus is not dramatic, the properties at break reduce by half as compared to neat

epoxy. As already explained in our previous work on these systems,²⁹ such decrease could be explained by the immiscibility of the blend constituents and problems in the manufacturing process. In fact, the introduction of the healing agent makes the degassing process more difficult, thus leaving more voids in the final blends. In these conditions, the quasi-static tensile properties at break are heavily impaired.

4.4 | Fracture behavior and evaluation of the healing efficiency

The fracture toughness of neat samples and of prepared blends was evaluated through three-point bending tests on notched specimens. Representative load–displacement curves from flexural tests on SENB samples under quasi-static conditions (virgin and healed samples) are collected in Figure 6(a–c), while the maximum load (P), critical stress intensity factor (K_{IC}) and critical strain energy release rate (G_{IC}) values are numerically summarized in Table 7. All the prepared blends are characterized by a brittle behavior, with a sudden drop of the load after first failure at P . From Figure 6(a) it can be seen that the increasing fraction of COC yields an increase in the fracture properties of the blends, in terms of maximum load (P) and extension at break, thus leading to an enhancement of the fracture resistance of the material (all the samples have approximately the same dimensions). The toughening effect provided by the COC particles within a fragile epoxy matrix, already detected in the past work,²⁹ is therefore confirmed. From Figure 6(b) and Figure 6(c) it can be seen that, thanks to the presence of COC particles within the epoxy matrix, the mending process results in a successful repair of the crack. As the fraction of healing agent increases, the load bearing capacity of the thermally mended specimen increases over the whole range of healing temperatures. On the contrary, neat epoxy resin after the mending process does not recover its structural integrity, and the healed samples do not show any load bearing capacity, regardless the mending temperature (see Table 7). From Figure 6(b), it can be seen that in epoxy/COC20 samples an increase of the healing temperature leads to a sensible increase of P , K_{IC} and G_{IC} values. For instance, K_{IC} passes from 0.82 $\text{MPa}\cdot\text{m}^{1/2}$ for the epoxy/COC20 sample healed at 145 °C up to 0.99 $\text{MPa}\cdot\text{m}^{1/2}$ for a healing temperature of 190 °C. In the epoxy/COC30 samples the mending temperature does not seem to strongly affect the fracture behavior of the material (see Figure 6(c)). It could be also interesting to note that the thermal treatment on unhealed samples leads to an interesting increase of both G_{IC} and K_{IC} , probably due to the further crosslinking of

Samples	T _{onset} (°C)	T _{50%} (°C)	T _{dEP} (°C)	T _{dCOC} (°C)	m ₇₀₀ (%)
u-EP	332.7	369.3	369.8	—	8.0
u-EP/COC20	335.2	284.1	355.2	473.2	5.2
u-EP/COC30	338.7	403.5	367.7	478.0	5.5
u-COC	457.0	473.2	—	473.7	0.0
t ¹⁴⁵ -EP/COC20	338.8	388.4	362.7	476.0	5.4
t ¹⁶⁰ -EP/COC20	340.0	389.3	365.3	494.4	6.4
t ¹⁷⁵ -EP/COC20	339.6	387.1	367.2	481.0	5.2
t ¹⁹⁰ -EP/COC20	341.7	389.3	371.7	475.2	6.0
t ¹⁴⁵ -EP/COC30	338.8	406.8	371.8	478.0	5.2
t ¹⁶⁰ -EP/COC30	338.6	405.5	363.2	476.7	4.8
t ¹⁷⁵ -EP/COC30	340.9	407.0	363.0	480.5	5.2
t ¹⁹⁰ -EP/COC30	340.4	404.7	361.0	481.0	4.9

TABLE 5 Results of TGA tests on untreated epoxy and EP/COC blends

Note: T_{onset} is the onset degradation temperature; T_{50%} is the temperature associated to a mass loss of 50%. T_{dEP} is the decomposition temperature of epoxy matrix; T_{dCOC} is the decomposition temperature of COC; m₇₀₀ is the residual mass at 700°C.

TABLE 6 Quasi-static tensile and flexural properties of u-EP, u-EP/COC20, u-EP/COC30 samples

Samples	Tensile modulus (MPa)	Tensile stress at break (MPa)	Tensile strain at break (%)	Flexural modulus (MPa)	Flexural strength (MPa)	Flexural strain at break (%)
u-EP	3099.9 ± 6.3	56.8 ± 2.3	6.8 ± 0.6	2868.7 ± 105.4	125.5 ± 5.7	6.3 ± 0.3
u-EP/COC20	3002.0 ± 169.0	36.9 ± 3.6	3.5 ± 0.2	2917.9 ± 167.0	55.5 ± 3.6	2.1 ± 0.2
u-EP/COC30	2447.3 ± 198.0	25.4 ± 2.5	2.4 ± 0.2	2683.3 ± 214.8	42.3 ± 1.9	1.7 ± 0.1

the epoxy resin in the blends. For instance, untreated neat epoxy sample shows a K_{IC} value of 0.88 MPa·m^{1/2}, while the epoxy/COC30 blend treated at 190°C has a K_{IC} of 1.40 MPa·m^{1/2}. The results reported in our previous work are therefore confirmed,²⁹ and COC introduction seems to considerably improve the fracture behavior before and after the healing process. Moreover, with a COC content of 20 wt% the temperature at which the healing process is performed seems to affect the healing capability, while increasing the COC amount up to 30 wt% a decrease of the mending temperature does not seem to promote a substantial drop of the fracture properties in the healed samples.

The same trends can be detected also if the samples repaired two times are considered (see Table 7). It can be hypothesized that, at limited COC amounts, the viscosity drop at elevated healing temperature plays an important role in the diffusion of the healing agent in the crack zone. On the contrary, at elevated COC contents the crack filling process is less dependent on the viscosity of the healing agent, due to the higher availability of COC particles near the crack area.

In order to better visualize the effect of the COC content and of the healing temperature, K_{IC} values of the thermally treated and healed samples are compared in Figure 7(a-b) for the epoxy/COC20 and epoxy/COC30 blends, respectively. Even from Figure 7(a) it can be seen that a decrease of the healing temperature in the epoxy/COC20 blends leads to a slight drop of the K_{IC} values. It is also interesting to note that a second healing process does not lead to a decrease of the fracture toughness of the materials, if compared with the samples healed only one time. Considering the standard deviation values, it can be appreciated that the treatment temperature does not substantially influence K_{IC} values of virgin samples. For a COC content of 30 wt% (see Figure 7(b)), the K_{IC} values in the healed samples are less affected by the mending temperature, and even in this case a second healing process does not lead to significant variations of the fracture toughness of the materials.

It is also important to provide a numerical estimation of the healing efficiency of the prepared blends, distinguishing also the effect of the healing temperature

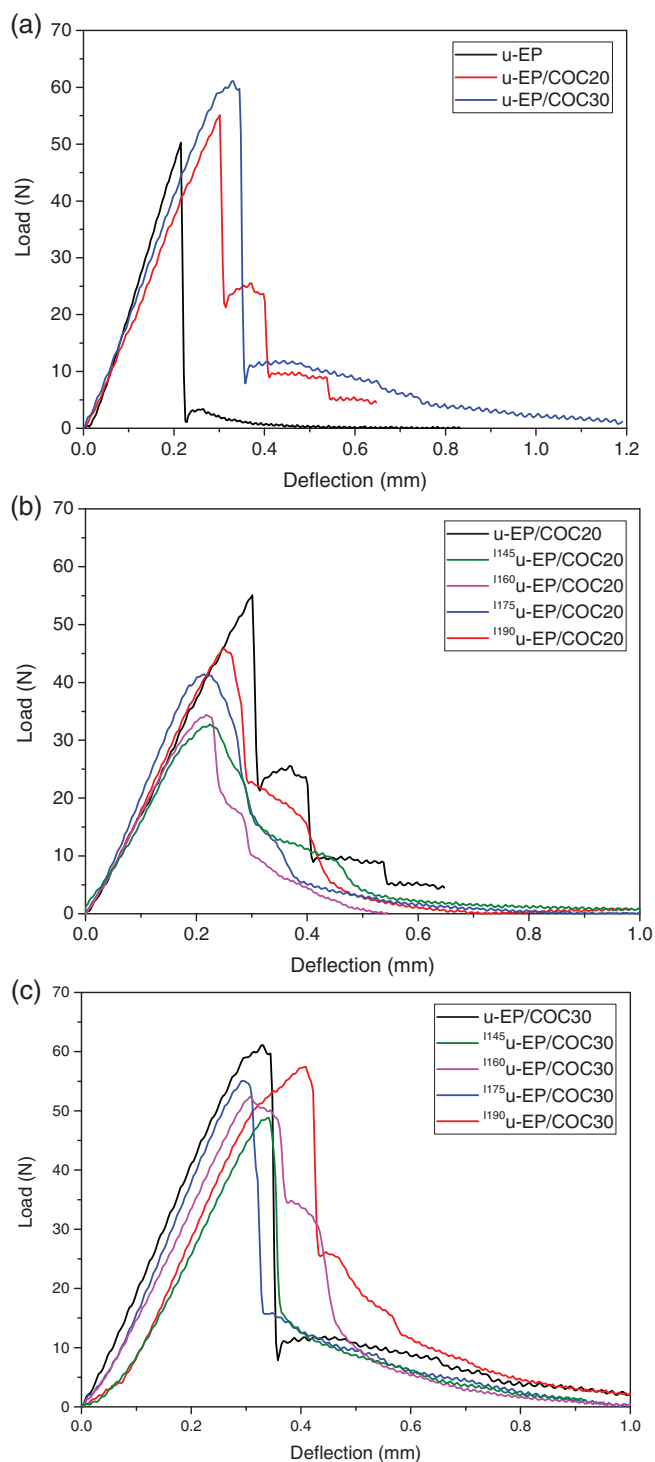


FIGURE 6 Representative load–displacement curves from fracture tests on SENB samples. (a) u-EP, u-EP/COC20, and u-EP/COC30 samples; (b) u-EP/COC20 samples healed at different temperatures; (c) EP/COC30 samples healed at different temperatures. COC, cyclic olefin copolmer; EP, epoxy; SENB, single edge notched beam [Color figure can be viewed at wileyonlinelibrary.com]

from that played by the thermal treatment on the epoxy matrix. Figure 8 demonstrates the apparent (η) and real

(η') healing efficiency values at different mending temperatures for the prepared blends. It could be important to remind that considering the apparent healing efficiency (η) it is possible to take into account both the effect of the curing process of epoxy resin and the healing effect due to the presence of COC. On the other hand, analyzing real healing efficiency values (η'), the mending potential of COC is the only factor taken into consideration. From the results of fracture toughness tests collected both in the first and in the second healing process, it can be seen that η values of EP/COC30 samples are systematically higher than those of the corresponding EP/COC20 blends, regardless to the healing temperature. This can be probably attributed to the higher availability of COC domains within the crack zone. Considering the samples healed only one time, in EP/COC20 blends both η and η' values increase with the healing temperature. For instance, η of the EP/COC20 sample increases from 66.3% up to 82.3% as the temperature rises from 145 °C up to 190 °C. This effect is much less pronounced if EP/COC30 blends are considered. It should be noted that for EP/COC30 blends, the healing efficiencies did not decrease substantially compared to EP/COC20. In fact, compared to previous work,²⁹ efficiency values for EP/COC30 at lowest mending temperature, that is 145 °C are remarkably close which means optimized conditions have been detected by this work. The last consideration is valid also if η values in the second healing process are considered. It is also interesting to note that η values in the second healing process are slightly higher than that observed in the first healing cycles, regardless the healing temperature or to the COC content. This could be explained considering that probably the crack path in the second test is the same of the first one. In these conditions, the interdiffusion of the softened COC phase within the crack plane during the second healing process is favored.

Considering standard deviation values, it can be generally seen that η' is quite similar to η in the epoxy/COC20 blends, and that increasing the COC amount up to 30 wt% η' values result to be only slightly lower than the corresponding η results. This suggests that in these blends the healing process takes place mainly because of the diffusion of the COC particles in the crack plane, while the positive effect of the thermal treatment on the fracture properties of the epoxy matrix plays a minor role.

Optical micrographs of the EP/COC20 samples repaired one time at different temperatures are reported in Figure 9(a–d). In all the samples, COC microparticles softened and penetrated in the cracks during the healing process. This means that the applied healing

P (N)					
Sample	Virgin	190 °C	175 °C	160 °C	145 °C
u-EP	51.0 ± 3.7	13 ± 7.4	—	—	—
^I u-EP/COC20	56.0 ± 3.7	44.0 ± 3.1	44.0 ± 7.6	36.0 ± 3.3	36.0 ± 3.8
^{II} u-EP/COC20	56.0 ± 3.7	45.0 ± 7.8	45.0 ± 2.1	34.0 ± 5.8	30.0 ± 7.3
t-EP/COC20	—	46.1 ± 1.7	47.0 ± 5.7	44.0 ± 6.5	44.0 ± 4.4
^I u-EP/COC30	58.0 ± 1.2	55.0 ± 5.0	50.0 ± 9.1	52.0 ± 8.8	48.0 ± 3.1
^{II} u-EP/COC30	58.0 ± 1.2	59.0 ± 8.4	50.0 ± 9.8	52.0 ± 8.3	44.0 ± 3.7
t-EP/COC30	—	65.0 ± 12.9	58.0 ± 13.4	58.0 ± 6.3	55.0 ± 6.6
K _{IC} (MPa·m ^{1/2})					
Sample	Virgin	190°C	175°C	160°C	145°C
u-EP	0.88 ± 0.04	0.23 ± 0.11	—	—	—
^I u-EP/COC20	1.24 ± 0.11	0.99 ± 0.09	0.99 ± 0.24	0.83 ± 0.09	0.85 ± 0.12
^{II} u-EP/COC20	1.24 ± 0.11	0.98 ± 0.17	1.01 ± 0.13	0.80 ± 0.15	0.71 ± 0.14
t-EP/COC20	—	1.09 ± 0.05	1.15 ± 0.18	1.03 ± 0.20	1.02 ± 0.16
^I u-EP/COC30	1.26 ± 0.12	1.20 ± 0.07	1.14 ± 0.08	1.14 ± 0.04	1.19 ± 0.12
^{II} u-EP/COC30	1.26 ± 0.12	1.29 ± 0.14	1.14 ± 0.11	1.13 ± 0.07	1.08 ± 0.16
t-EP/COC30	—	1.40 ± 0.21	1.39 ± 0.29	1.40 ± 0.05	1.36 ± 0.06
G _{IC} (kJ·m ⁻²)					
Sample	Virgin	190°C	175°C	160°C	145°C
u-EP	0.39 ± 0.07	0.04 ± 0.02	—	—	—
^I u-EP/COC20	0.56 ± 0.05	0.36 ± 0.07	0.35 ± 0.06	0.29 ± 0.05	0.30 ± 0.07
^{II} u-EP/COC20	0.56 ± 0.05	0.32 ± 0.14	0.34 ± 0.06	0.29 ± 0.05	0.20 ± 0.04
t-EP/COC20	—	0.37 ± 0.05	0.43 ± 0.15	0.38 ± 0.12	0.40 ± 0.13
^I u-EP/COC30	0.72 ± 0.08	0.73 ± 0.18	0.52 ± 0.06	0.52 ± 0.02	0.51 ± 0.06
^{II} u-EP/COC30	0.72 ± 0.08	0.74 ± 0.07	0.48 ± 0.13	0.49 ± 0.02	0.40 ± 0.08
t-EP/COC30	—	0.75 ± 0.13	0.68 ± 0.16	0.62 ± 0.11	0.57 ± 0.03

TABLE 7 P, K_{IC}, and G_{IC} values from fracture tests on untreated, repaired and treated blends

temperatures were high enough to soften the COC phase. Thanks to the good particle dispersion in the matrix, COC filled the empty space in crack region, hence bridging the crack fronts. In this way, the broken specimens were thermally mended. In fact, the crack is clearly visible at the center of the four images, and a thin dark line suggests the presence of thermoplastic COC that flowed into the crack and mended the material. In all the samples, the crack surface appears homogeneously filled and a rather good adhesion can be observed between the two polymeric phases. In some zones of the micrographs, the presence of repaired cracks with some empty spaces can be noticed. This could be associated to unavailability of healing agent, along with the fact that epoxy cannot repair by itself. In these conditions, it can be hypothesized that a second mending could easily occur in the same region, because COC is already present near the crack line. A second mending process would only involve softening and solidification of COC, and the softened

healing agent would not have to flow through the matrix to reach the fracture region.

After the first healing process, the samples were broken again during fracture tests in three-point bending configuration. Optical microscopy was then performed on these samples to detect variations in the crack formation before and after the healing process. Micrographs of the polished surfaces of healed and fractured EP/COC20 samples are reported in Figure 10(a–d). In these figures, the healing was performed at different temperatures. It is interesting to notice that the fracture in the first crack process propagates both through the epoxy and through the COC domains, and no interfacial debonding can be detected between the epoxy and COC phase. It is also interesting to notice that, regardless to the mending temperature, in the second breaking operation the crack passes through the path followed in the first healing process. Therefore, COC particles can be seen around the cracks: the material has flown from these

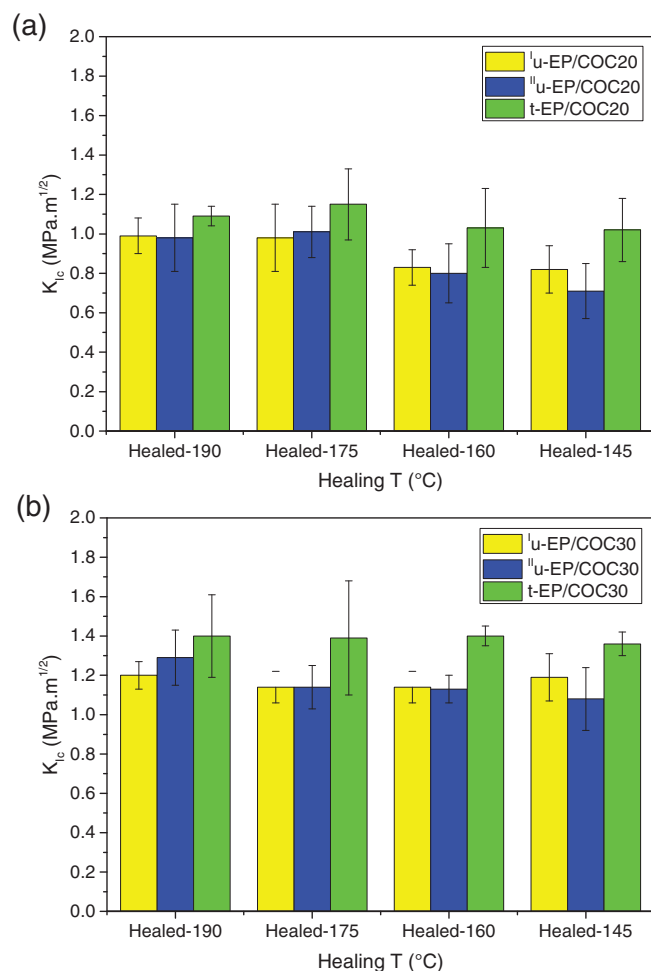


FIGURE 7 Trends of K_{IC} at different mending temperatures for healed and treated (a) EP/COC20 and (b) EP/COC30 samples. COC, cyclic olefin copolymer; EP, epoxy [Color figure can be viewed at wileyonlinelibrary.com]

particles to the crack surface during the first healing. Such microstructural feature could explain why the healing efficiency values in the second mending process are generally higher than those observed in the first repair stage.

5 | CONCLUSIONS

An amorphous COC was used as healing agent for an epoxy resin, with the aim to evaluate the effect of the mending temperature (from 145 up to 190°C) on its healing capability. Optical microscope images revealed that, COC domains were homogeneously dispersed within the epoxy regardless their concentration. COC addition enhanced the degradation resistance of the samples, as observed through TGA tests, while the decrease of the mechanical properties with respect to neat epoxy, experienced both in flexural and in tensile mode, was attributed to the immiscibility of the two polymer phases and to a

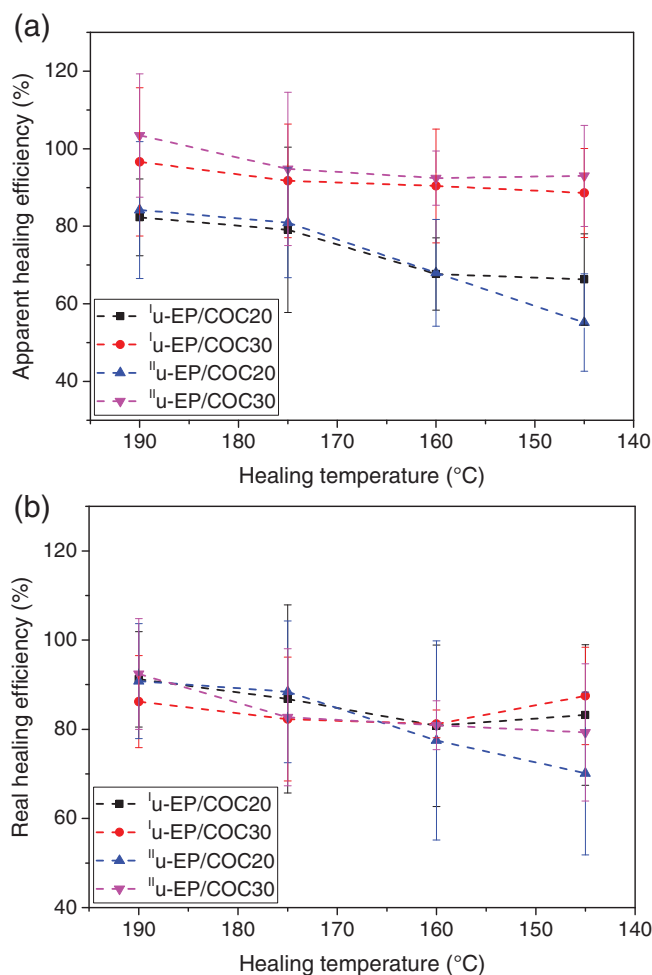


FIGURE 8 (a) Apparent and (b) real healing efficiencies of EP/COC blends at different temperature. COC, cyclic olefin copolymer; EP, epoxy [Color figure can be viewed at wileyonlinelibrary.com]

rather low interfacial interaction. COC addition was responsible of an enhancement of the fracture toughness, coupled with a remarkable healing capability, even at limited COC amounts (i.e. 20 wt%) and low mending temperature (i.e., 145°C). Multiple healing events were possible for these materials, and for a COC content of 30 wt% the healing efficiency did not seem to be impaired by the decrease of the repair temperature. In fact, efficiencies obtained were appreciably close or even higher compared to previous work with elevated mending parameters.²⁹ Optical microscope images revealed that the elevated values of healing efficiency could be attributed to the effective flow of the softened COC phase through the crack zone, even at low mending temperatures.

ACKNOWLEDGMENTS

This research activity has been financed by the Fondazione Cassa di Risparmio di Trento e Rovereto (CARITRO, Grant number 2017.0389) within the project

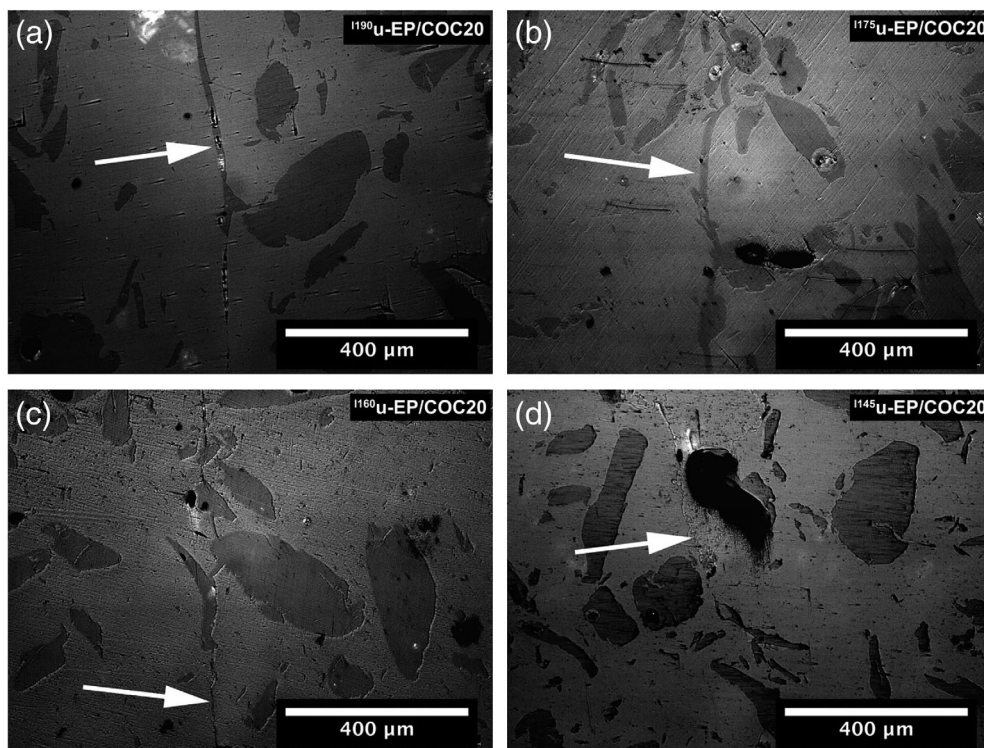


FIGURE 9 Optical microscope images of the polished surfaces of healed samples. (a) $^{1190}\text{u-EP/COC20}$, (b) $^{1175}\text{u-EP/COC20}$, (c) $^{1160}\text{u-EP/COC20}$, (d) $^{1145}\text{u-EP/COC20}$. COC, cyclic olefin copolmer; EP, epoxy

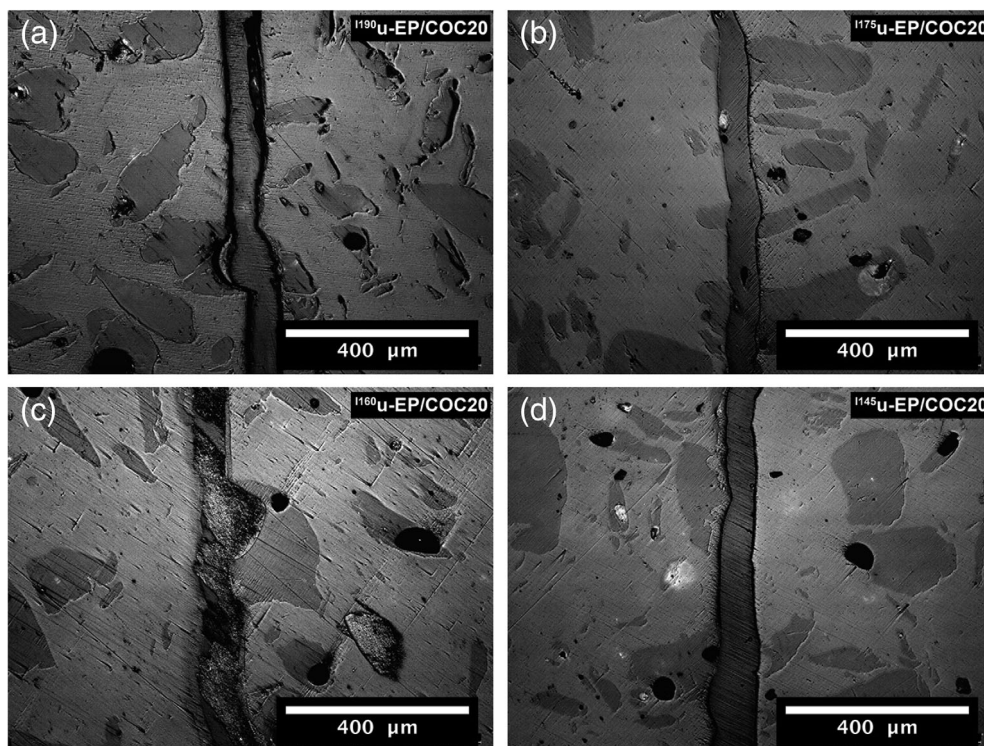


FIGURE 10 Optical microscope images of the fracture front in the broken samples, previously healed at different temperatures. (a) $^{1190}\text{u-EP/COC20}$, (b) $^{1175}\text{u-EP/COC20}$, (c) $^{1160}\text{u-EP/COC20}$, (d) $^{1145}\text{u-EP/COC20}$. COC, cyclic olefin copolmer; EP, epoxy

“Development of self-sensing/self healing structural composites using graphene treated fibers”. The work has been also supported by the National Interuniversity

Consortium of Materials Science and Technology (INSTM). Mr. Matteo Berzacola is gratefully acknowledged for his support to the experimental work.

ORCID

Andrea Dorigato  <https://orcid.org/0000-0002-4743-7192>

Haroon Mahmood  <https://orcid.org/0000-0003-3572-5004>

Alessandro Pegoretti  <https://orcid.org/0000-0001-9641-9735>

REFERENCES

- [1] A. Dorigato, A. Pegoretti, M. Quaresimin, *Mater. Sci. Eng., A* **2011**, 528, 6324.
- [2] A. Dorigato, S. Morandi, A. Pegoretti, *J. Compos. Mater.* **2011**, 46, 1439.
- [3] D. Pedrazzoli, A. Dorigato, A. Pegoretti, *Composites, Part A* **2012**, 43, 1285.
- [4] D. Pedrazzoli, A. Dorigato, A. Pegoretti, *J. Nanosci. Nanotechnol.* **2012**, 12, 4093.
- [5] H. Mahmood, A. Dorigato, A. Pegoretti, *Fibers* **2019**, 7, 17.
- [6] O. Shishkina, V. Romanov, Y. Abdin, S. V. Lomov, L. Gorbatiikh, *Compos. Interfaces* **2018**, 26, 507.
- [7] R. V. S. P. Sanka, B. Krishnakumar, Y. Leterrier, S. Pandey, S. Rana, V. Michaud, *Front. Mater.* **2019**, 6, 1.
- [8] V. K. Thakur, M. R. Kessler, *Polymer* **2015**, 69, 369.
- [9] I. L. Hia, V. Vahedi, P. Pasbakhsh, *Polym. Rev.* **2016**, 56, 225.
- [10] M. Scheiner, T. J. Dickens, O. Okoli, *Polymer* **2016**, 83, 260.
- [11] W. H. Binder, *Self-Healing Polymers: From Principles to Applications*, Wiley, Weinheim, Germany **2013**.
- [12] S. R. White, N. R. Sottos, P. H. Geubelle, J. S. Moore, M. R. Kessler, S. R. Sriram, E. N. Brown, S. Viswanathan, *Nature* **2001**, 409, 794.
- [13] B. J. Blaiszik, S. L. B. Kramer, S. C. Olugebefola, J. S. Moore, N. R. Sottos, S. R. White, *Annu. Rev. Mater. Res.* **2010**, 40, 179.
- [14] D. Y. Zhu, M. Z. Rong, M. Q. Zhang, *Prog. Polym. Sci.* **2015**, 175, 49.
- [15] A. Cohades, C. Branfoot, S. Rae, I. Bond, V. Michaud, *Adv. Mater. Interfaces* **2018**, 5, 1800177.
- [16] S. Dello Iacono, A. Martone, A. Pastore, G. Filippone, D. Acierno, M. Zarrelli, M. Giordano, E. Amendola, *Polym. Eng. Sci.* **2017**, 57, 674.
- [17] J. Nji, G. Li, *Smart Mater. Struct.* **2012**, 21, 025011.
- [18] K. Pingkarawat, C. H. Wang, R. J. Varley, A. P. Mouritz, *Composites, Part A* **2014**, 65, 10.
- [19] S. A. Hayes, W. Zhang, M. Branthwaite, F. R. Jones, *J. R. Soc., Interface* **2007**, 4, 381.
- [20] H. Birjandi Nejad, J. M. Robertson, P. T. Mather, *MRS Commun.* **2015**, 5, 211.
- [21] C. H. Wang, K. Sidhu, T. Yang, J. Zhang, R. Shanks, *Composites, Part A* **2012**, 43, 512.
- [22] C. Dell'Olio, Q. Yuan, R. J. Varley, *Macromol. Mater. Eng.* **2015**, 300, 70.
- [23] X. Luo, R. Ou, D. E. Eberly, A. Singhal, W. Viratyaporn, P. T. Mather, *ACS Appl. Mater. Interfaces* **2009**, 1, 612.
- [24] E. D. Rodriguez, X. Luo, P. T. Mather, *ACS Appl. Mater. Interfaces* **2011**, 3, 152.
- [25] X. Luo, P. T. Mather, *ACS Macro Lett.* **2013**, 2, 152.
- [26] S. Meure, D. Y. Wu, S. Furman, *Acta Mater.* **2009**, 57, 4312.
- [27] K. Pingkarawat, T. Bhat, D. A. Craze, C. H. Wang, R. J. Varley, A. P. Mouritz, *Polym. Chem.* **2013**, 4, 5007.
- [28] H. Wei, Y. Yao, Y. Liu, J. Leng, *Composites, Part B* **2015**, 83, 7.
- [29] H. Mahmood, A. Dorigato, A. Pegoretti, *Express Polym. Lett.* **2020**, 14, 368.
- [30] A. Dorigato, A. Pegoretti, L. Fambri, M. Slouf, J. Kolarik, *J. Appl. Polym. Sci.* **2011**, 119, 3393.
- [31] A. Biani, A. Dorigato, W. Bonani, M. Slouf, A. Pegoretti, *Express Polym. Lett.* **2016**, 10, 977.
- [32] A. Pegoretti, A. Dorigato, A. Biani, M. Slouf, *J. Mater. Sci.* **2016**, 51, 3907.
- [33] A. Dorigato, A. Biani, W. Bonani, A. Pegoretti, *J. Cell. Plast.* **2019**, 55, 263.
- [34] Y. Yao, J. Wang, H. Lu, B. Xu, Y. Fu, Y. Liu, J. Leng, *Smart Mater. Struct.* **2016**, 25, 015021.
- [35] A. Cohades, E. Manfredi, C. J. G. Plummer, V. Michaud, *Eur. Polym. J.* **2016**, 81, 114.
- [36] J. Karger-Kocsis, *Polym. Bull.* **2016**, 73, 3081.
- [37] H. Mahmood, A. Dorigato, A. Pegoretti, *Materials* **2020**, 13, 2165.
- [38] H. A. Mannan, H. Mukhtar, T. Murugesan, R. Nasir, D. F. Mohshim, A. Mushtaq, *Chem. Eng. Technol.* **2013**, 36, 1838.
- [39] A. Dorigato, A. Pegoretti, L. Fambri, C. Lonardi, M. Slouf, J. Kolarik, *Express Polym. Lett.* **2011**, 5, 23.
- [40] M. Buccella, A. Dorigato, E. Pasqualini, M. Caldara, L. Fambri, *J. Polym. Res.* **2012**, 19, 9935.
- [41] D. Rigotti, A. Dorigato, A. Pegoretti, *Mater. Today Commun.* **2018**, 15, 228.
- [42] Y. Li, H. Shimizu, *Macromol. Biosci.* **2007**, 7, 921.
- [43] V. Nagarajan, A. K. Mohanty, M. Misra, *Polym. Eng. Sci.* **2018**, 58, 280.
- [44] Y. Guo, X. Zuo, Y. Xue, Y. Zhou, Z. Yang, Y.-C. Chuang, C.-C. Chang, G. Yuan, S. K. Satija, D. Gersappe, M. H. Rafailovich, *Macromolecules* **2018**, 51, 3897.
- [45] Y. C. Ching, C. H. Chuah, K. Y. Ching, L. C. Abdullah, A. Rahman, in *Recent Developments in Polymer Macro, Micro and Nano Blends* (Eds: P. M. Visakh, G. Markovic, D. Pasquini), Woodhead Publishing, Sawton, UK **2017**.
- [46] J. Karger-Kocsis, *Polypropylene Structure, blends and Composites*, Springer, Netherlands **1995**.
- [47] L. A. Utracki, P. Mukhopadhyay, R. Gupta, K. in *Polymer Blends Handbook* (Eds: L. A. Utracki, C. A. Wilkie), Springer Netherlands, Dordrecht **2014**.
- [48] A. E. Krauklis, A. T. Echtermeyer, *Polymers* **2018**, 10, 1017.
- [49] ASTM, S.,S test methods for plane-strain fracture toughness and strain energy release rate of plastic materials.

SUPPORTING INFORMATION

Additional supporting information may be found online in the Supporting Information section at the end of this article.

How to cite this article: Dorigato A, Mahmood H, Pegoretti A. Optimization of the thermal mending process in epoxy/cyclic olefin copolymer blends. *J Appl Polym Sci.* 2021;138: e49937. <https://doi.org/10.1002/app.49937>